Linear antiferrodistortive-antiferromagnetic effect in multiferroics: Physical manifestations

Anna N. Morozovska, Victoria V. Khist, Maya D. Glinchuk, Venkatraman Gopalan, and Eugene A. Eliseev

Linear antiferrodistorsive-antiferromagnetic effect in multiferroics: physical manifestations

Anna N. Morozovska[1], Victoria V. Khist[2], Maya D. Glinchuk[3], Venkatraman Gopalan[4*],
Eugene A. Eliseev [3†]

[1]Institute of Physics, National Academy of Sciences of Ukraine,

46, pr. Nauky, 03028 Kyiv, Ukraine

[2] National University of Water Management and Nature Resources Use,

Rivne, 33028, st. Soborna, 11, Ukraine

[3] Institute for Problems of Materials Science, National Academy of Sciences of Ukraine,

3, Krjijanovskogo, 03142 Kyiv, Ukraine

[4] Department of Materials Science and Engineering, Pennsylvania State University, University

Park, PA 16802, USA

Abstract

Using the theory of symmetry and the microscopic model we predicted the possibility of a linear antiferrodistortive-antiferromagnetic effect in the perovskites with structural antiferrodistortive and antiferromagnetic long-range ordering and found the necessary conditions of its occurrence. The main physical manifestations of this effect are the smearing of the antiferromagnetic transition and the jump of the specific heat near it. In the absence of external fields linear antiferrodistortive-antiferromagnetic coupling can induce a weak antiferromagnetic ordering above the Neel temperature, but below the temperature of antiferrodistortive transition. Therefore, there is the possibility of observing weak improper antiferromagnetism in multiferroics such as bismuth ferrite ($BiFeO_3$) at temperatures $T>T_N$, for which the Neel temperature T_N is about 645 K, and the antiferrodistortive transition temperature is about 1200 K. By quantitative comparison with experiment we made estimations of the linear antiferrodistortive-antiferromagnetic effect in the solid solutions of multiferroic $Bi_{1-x}R_xFeO_3$ (R=La, Nd).

---

[*] Corresponding author: vgopalanpsu@gmail.com

[†] Corresponding author: eugene.a.eliseev@gmail.com

1. Introduction

Multiferroics, generally defined as ferroics with several types of long-range order interacting with each other, are unique model systems for fundamental physical studies of versatile couplings between the spontaneous polarization, magnetization, structural and antiferromagnetic order parameters [1, 2, 3, 4]. The most well-known and important effect for applications of multiferroics is the magnetoelectric coupling between the polarization and magnetization, through which one can write information by an electric field and readout it by a magnetic field [1, 4, 5].

Given the unique importance of multiferroics for wide variety of applications, other types of couplings are actively investigated in antiferrodistortive multiferroics in addition to the magnetoelectric coupling [6, 7, 8, 9, 10]. The couplings are associated with the presence of structural order parameter and its gradient. In the case of a inhomogeneous distribution of the order parameter, which is inevitable near the surface or in the presence of developed domain structure of ferroelectric, magnetic or structural types, there is a coupling between the various order parameters and their gradients [6-10]. Therefore, according to the theory of symmetry, the flexoelectric-antiferrodistortive and antiferrodistortive-flexoelectric coupling between structural, polar and magnetic order parameters [11, 12, 13] can exist in antiferrodistortive multiferroics in addition antiferrodistortive-magnetic and antiferrodistortive-electrical coupling [14, 15]. In the work the term "antiferrodistortive symmetry" means only rotational symmetry of the oxygen octahedra MO_6 with respect to the cube A_8 in antiferrodistortive perovskites with the structural formula AMO_3. Oxygen atoms are displaced with respect to the centers of the cube faces A_8 in the antiferrodistortive phase, the angle or the value of the corresponding displacement is a structural order parameter (see e.g. [16]).

Coupling between the various orders parameters can be bilinear, linear-quadratic and biquadratic in the order parameters powers, depending on the extent to which the relevant parameter (or gradient) is proportional to the physical effect it has generated [1]. Biquadratic effects exist for arbitrary symmetry of multiferroic [17, 18, 19, 20], but the values of the corresponding tensor coupling constants strongly depend on its shape and size [21]. The appearance of non-zero bilinear effects is material-specific, they are determined by the spatial magnetic and antiferrodistortive- symmetry of the material (see e.g. [4, 7, 14]). Consequently bilinear effects are significantly less common, but their physical manifestations can be much more strong and non-trivial, rather than the manifestations of biquadratic effects [4]. Perhaps that is why researchers are actively "hunting" for bilinear coupling effects in multiferroics.

In this work we predicted the possibility of linear antiferrodistortive-antiferromagnetic coupling existence in perovskites with antiferrodistortive and antiferromagnetic ordering and

found the necessary conditions of the coupling occurrence. Also we discuss the main physical manifestations of the effect, such as the smearing of antiferromagnetic (AFM) transition, specific heat jump near the transition and weak antiferromagnetism above the Neel temperature. We chose multiferroic bismuth ferrite ($BiFeO_3$) as the model material.

Our choice of $BiFeO_3$ is based on the fact that the material is one of the most promising multiferroic with a relatively high magnetoelectric coupling coefficient; it reveals antiferrodistortive order at temperatures below 1200 K; is ferroelectric with a high spontaneous polarization below 1100 K and antiferromagnetic below Neel temperature $T_N \approx (640 - 650)$ K [4, 22]. Despite the great amount of experimental studies on the $BiFeO_3$ multiferroic properties [23, 4, 5], many important issues remain unclear in the sense of understanding of the physical mechanisms responsible for the emergence and manifestation of these properties [22]. In other words, the theoretical description of $BiFeO_3$ physical properties is far behind the experiment. In particular *ab initio* calculations, which allow determining the parameters of antiferrodistortive and antiferromagnetic subsystems, magnetoelectric, antiferrodistortive-magnetic and antiferrodistortive-electric couplings of the corresponding long-range order parameters with each other in $BiFeO_3$, are absent to date. On the other hand reliable experimental results, which analyses, as we will show below, allow making conclusions about the exclusive importance of the antiferrodistortive-type couplings in $BiFeO_3$.

Before presenting the problem statement and original results, let us make some comments about chosen research methods. As we discuss the principal possibility of a new kind of interaction between two long-range order parameters (antiferrodistortive and antiferromagnetic) in the bulk of multiferroic, in order to establish the existence of a particular interaction between the order parameters and unambiguously define the structure of corresponding material tensor, one can use the theory of symmetry, if its spatial and magnetic symmetry group is known [14]. Functional form of the antiferrodistive-antiferromagnetic coupling contribution to the free energy and its effect on phase transitions in multiferroics can be established within the framework of the continuous medium mean-field Ginzburg-Landau theory [11, 13]. However, it is impossible to define the value of the coupling strength, i.e. to calculate non-zero coupling constant for a given material, using phenomenological approach and the theory of symmetry. One can estimate the strength of antiferrodistive-antiferromagnetic coupling either from first principle quantum mechanical calculations within a specific microscopic model, or from the fitting to experimental data. Both of these approaches are indispensable to determine the coupling constants and complement each other well, but by themselves they are not free from drawbacks. Most of the first principle calculations (such as carried out in the framework of DFT) do not take into account correctly inhomogeneous long-range depolarization electric field in ferroics and the totality of the structural and magnetic antiferrodistortive modes, as well as do

not allow to say anything about the temperature dependence of the coupling constants. However it is possible to extract the coupling constant from the experiment sufficiently precisely and unambiguously, if the contribution of other effects is known within error margins.

In the work we consider step-by-step the microscopic picture necessary for the occurrence of linear antiferrodistortive-antiferromagnetic coupling in antiferrodistortive antiferromagnets with the structural formula AMO_3, establish the transformation law of linear antiferrodistortive-antiferromagnetic effect tensor, find its nonzero components of the theory of symmetry and estimate its numerical value from the smearing of specific heat jump near AFM transition for bismuth ferrite and its solid solutions $Bi_{1-x}R_xFeO_3$ (R=La, Nd).

2. Microscopic model for bilinear antiferrodistortive-antiferromagnetic coupling appearance

The antiferromagnetic order parameter of the two-sublattice antiferromagnet is an axial vector $\mathbf{L}$, that is equal to the difference of magnetization vectors of magnetic atoms in two equivalent sub-lattices A and B, $\mathbf{L} = (\mathbf{M}_A - \mathbf{M}_B)/2$, $\mathbf{M}_A = \sum_{i=1}^{A} g\mu_B \mathbf{S}_i$ и $\mathbf{M}_B = \sum_{i=1}^{B} g\mu_B \mathbf{S}_i$ (see **Figure 1a**). The antiferrodistortive order parameter is an axial vector, which is the angle of oxygen octahedra tilt φ. Below we use the equivalent form of order parameters defined as the oxygen displacement from symmetric position $\Phi = a \tan \varphi$, which can be calculated as the product of pseudocubic lattice constant a with tangent of angle φ. As a rule, the angle φ changes its sign in neighbouring cells, related to different sublattices A and B, namely $\mathbf{\Phi}_A = -\mathbf{\Phi}_B \equiv \mathbf{\Phi}$. The contribution of bilinear antiferrodistortive-magnetic coupling into the free energy is described be the following expression:

$$g_{RM}^L = \frac{\chi_{ij}}{2}\left(M_{Ai}\Phi_{Aj} + M_{Bi}\Phi_{Bj}\right) \equiv \frac{\chi_{ij}}{2}\left(M_{Ai} - M_{Bi}\right)\Phi_j \equiv \chi_{ij}L_i\Phi_j \qquad (1a)$$

Equation (1a) should be invariant under the translation on the basic vector of pseudocubic lattice, since magnetization vectors of each sublattices $\mathbf{M}_j$ change their signs, and the sublattice A transforms into the sublattice B under such translation, therefore vector $\mathbf{\Phi}$ also changes its sign and from the macroscopic point of view nothing changes in the system. Thus the necessary condition for the linear antiferrodistortive-antiferromagnetic effect appearance is the simultaneous sign change of the vectors components M_i and Φ_j in the neighbouring sublattices A and B. Otherwise the corresponding component χ_{ij} of the antiferrodistortive-antiferromagnetic tensor is identically zero in a high temperature parent phase, i.e. is becomes zero everywhere as it follows from the free energy expansion continuity on the irreducible representation of the

parent phase. The same speculations lead us to the conclusion about impossibility of the nonzero linear antiferrodistortive-ferromagnetic term $\chi_{ij}M_i\Phi_j$ appearance.

Equation (1a) should be invariant under the time-reversal operation **T** and therefore the transformation law of the linear antiferrodistortive-antiferromagnetic effect tensor components χ_{ij} under the point group symmetry operations with the matrix elements, C_{ij}, has the form $\chi_{ij} = (-1)^{tr} C_{im}C_{jk}\chi_{mk}$. The transformation laws of the order parameters are $\Phi_k = \det(C)C_{kf}\Phi_f$ and $L_i = (-1)^{tr}\det(C)C_{ip}L_p$. Determinant $\det(C) = \pm1$; the factor tr denotes either the presence ($tr = 1$) or the absence ($tr = 0$) of the time-reversal operation. Here the summation is performed over the repeating indexes. As it follows directly from the transformation law of χ_{ij}, it is **T**-odd tensor (similarly to L_i that is T-odd vector). The T-properties of the bilinear antiferrodistortive-antiferromagnetic coupling tensor χ_{ij} are the similar to the properties of piezomagnetic tensor. Thus, simply rephrasing Landau and Lifshitz speculations for a piezomagnetism [24], the antiferrodistortive-antiferromagnetic coupling is possible only in materials with a magnetic structure, since without it the properties are invariant under the transformation **T**, and therefore the effect can exist in antiferromagnets belonging to certain magnetic symmetry classes which contain **T** only in combination with rotations or reflections, or else, do not contain **T** at all [25].

Since χ_{ij} is identically zero in materials without a magnetic structure, it can be proportional to the sublattice magnetization or to the antiferromagnetic order parameter, or to some other order parameter, as it can be for a linear magnetoelectric [26] or piezoelectric [27] tensors. However it is only a possibility, but not a mandatory condition that follows from a symmetry theory. To illustrate this, a well-known analogy with a piezoelectric effect tensor can be used [24]. The latter can exist in any material without a space inversion (quartz, gallium nitride, zinc oxide, etc), but not only in a polar phase of ferroelectrics being proportional to the spontaneous polarization. That is why we decided not to limit ourselves by the case when χ_{ij} is proportional to antiferromagnetic order parameter, instead we would like to underline that the trilinear antiferrodistortive-antiferromagnetic coupling, described by invariants $\chi_{ijkl}L_i\Phi_j\Phi_k\Phi_l$ are $\tilde{\chi}_{ijkl}L_iL_jL_k\Phi_l$, should appear simultaneously with the bilinear antiferrodistortive-antiferromagnetic coupling considered above, as well as higher odd order couplings of the type. Below we will concentrate on the study of the bilinear antiferrodistortive-antiferromagnetic coupling (1a) physical manifestations, since assume that the bilinear effect should dominate over the higher order odd ones under the same other conditions.

For the magnetic and spatial symmetry groups corresponding to $BiFeO_3$ (spatial group is $R\bar{3}c$, magnetic group is $\bar{3}m$ or $I^-3_z^+2_x^+$ [28]), nonzero components of χ_{ij} are

$$\chi_{11}^{BiFeO3} = \chi_{22}^{BiFeO3} \neq \chi_{33}^{BiFeO3}. \tag{1b}$$

Nonzero components for $EuTiO_3$ are $\chi_{12}^{EuTiO3} = -\chi_{21}^{EuTiO3}$.
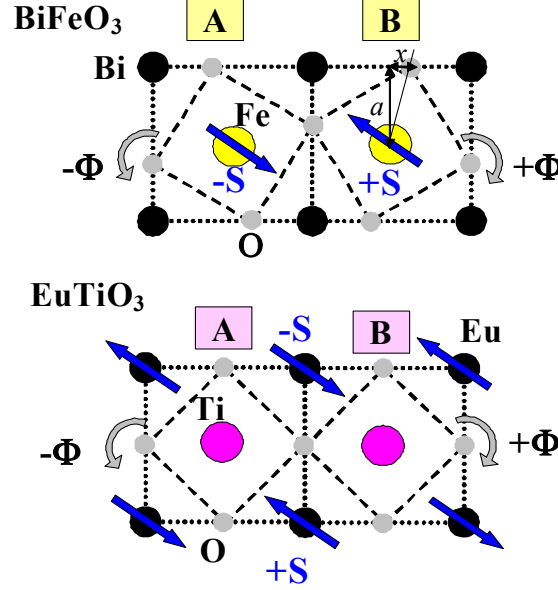
Figure 1. Schematic illustration to the microscopic model of the bilinear antiferrodistortive-antiferrodistortive coupling in the antiferrodistortive (AFD) phase of antiferromagnets with the structural formulae AMO_3. The tilt **Φ** and spin **S** local values should be opposite for the neighbouring oxygen octahedrons, as shown in the figure for $BiFeO_3$ and $EuTiO_3$.

3. Physical manifestations of the bilinear antiferrodistortive-antiferromagnetic coupling

Description of an antiferrodistortive antiferromagnet in the framework of the phenomenological free energy approach shows, that the bilinear antiferrodistortive-antiferromagnetic coupling, in the manifestations we are interested in, does not influence the behaviour of magnetic and dielectric susceptibilities in external magnetic or electric fields, i.e. the coupling is unrelated with magnetoelectric effect. Thus we can consider an antiferrodistortive antiferromagnet in the absence of external fields for the purposes of the study. For the sake of simplicity we regard that both antiferrodistortive and antiferromagnetic phase transitions are of the second order.

The expression for the free energy density of the uniform antiferrodistortive-antiferromagnet in the absence of external magnetic and electric fields in the isotropic 1D-approximation has the following form

$$g = g_{AFM} + g_{AFD} + g_{RM}^L, \tag{2a}$$

$$g_{AFM} = \frac{\alpha_L(T)}{2}L^2 + \beta_L\frac{L^4}{4}, \quad g_{AFD} = \frac{\alpha_\Phi(T)}{2}\Phi^2 + \frac{\beta_\Phi}{4}\Phi^4, \quad g_{RM}^L = \chi L\Phi \qquad (2b)$$

To describe the order parameters saturation behavior at low temperatures we used the quantum-corrected formula for the coefficient $\alpha_Q(T) = \alpha_{QT}T_Q\left(\coth(T_Q/T) - \coth(T_Q/T_q)\right)$ in Eqs.(2), which is valid in a wide temperature interval including low and high temperatures[29], where subscript $Q=L$ and the temperature T_q is equal to Neel temperature T_N of AFM parameter appearance; subscript $Q=\Phi$ and the temperature T_q is equal to AFD transition temperature T_S of the oxygen tilt appearance. At high temperatures $T \gg T_Q$ the formulae transforms into the classical limit, $\alpha_L(T) = \alpha_{LT}(T - T_N)$ and $\alpha_\Phi(T) = \alpha_{\Phi T}(T - T_S)$. Further let us solve the equations of state approximately in the assumption that the antiferrodistortive order parameter Φ appears at essentially higher temperatures T_S than the temperature T_N of spontaneous reversible antiferromagnetic order parameter L appearance. This allows us to make a decoupling approximation on the coupling coefficient χ. This is by the way a typical situation realizing for e.g. $Bi_{1-x}R_xFeO_3$ (R=La, Gd, Nd, x=0 – 0.2) with $T_N \approx (635 – 655)$ K and $T_S \approx 1200$ K [4, 28], $EuTiO_3$ with $T_N \approx 5$ K and $T_S \approx 280$ K [30, 31, 32].

Equations of state, $\partial g/\partial L = 0$ and $\partial g/\partial \Phi = 0$, contains built-in fields $\chi\Phi$ and χL correspondingly. As we have shown in the Supplement [33], the built-in fields leads to the antiferromagnetic (AFM) and antiferrodistortive (AFD) transition temperatures shifts, which are quadratic on the parameter χ, namely:

$$T_{AFM} = \frac{1}{2}(T_N + T_S) - \frac{1}{2}\sqrt{(T_S - T_N)^2 + \frac{\chi^2}{\alpha_{LT}\alpha_{\Phi T}}}, \qquad (3a)$$

$$T_{AFD} = \frac{1}{2}(T_N + T_S) + \frac{1}{2}\sqrt{(T_S - T_N)^2 + \frac{\chi^2}{\alpha_{LT}\alpha_{\Phi T}}}. \qquad (3b)$$

The shifts given by expressions (3) are relatively small under the validity of the strong inequality $\alpha_{LT}\alpha_{\Phi T}(T_S - T_N)^2 \gg \chi^2$. Under the simultaneous validity of the later inequality and the condition $T_N \ll T_S$ typical for antiferrodistortive antiferromagnets, expressions (3) can be simplified to the form, $T_{AFM} \approx T_N - \chi^2/(4\alpha_{LT}\alpha_{\Phi T}T_S)$ and $T_{AFD} \approx T_S + \chi^2/(4\alpha_{LT}\alpha_{\Phi T}T_S)$.

Besides the shift (3), built-in field $\chi\Phi$ leads to the smearing of the AFM order parameter L above the Neel transition temperature, i.e. in the paramagnetic phase. The smearing effect increases under the increase of χ value, as is shown in the **Figure 2a** by solid curves. Under the absence of linear coupling ($\chi=0$) one has $L = \pm\sqrt{\alpha_L(T)/\beta_L}$ at $T < T_N$. Structural order parameter

is practically independent on χ and equal to $\Phi(T) \approx \pm\sqrt{\alpha_{\Phi T}(T)/\beta_{\Phi}}$ (see dotted curve in **Figure 2a**).

Unfortunately, the antiferromagnetic order parameter L by itself is not directly observable, but some notion about its behavior can be obtained from the temperature dependences of neutron scattering and specific heat, if the contribution related with the long-range order appearance can be extracted. In particular the analyses and comparison with experiment of the specific heat changes $\delta C_P = -T\dfrac{d^2 g}{dT^2}$ allows us to verify the theoretical predictions made. In the typical case $T_{AFM} < T_{AFD}$ compact expression of the specific heat acquires the form:

$$\delta C_P = \begin{cases} -T\dfrac{d}{dT}\left(\dfrac{d\alpha_L}{dT}\dfrac{L^2}{2} + \dfrac{d\alpha_{\Phi}}{dT}\dfrac{\Phi^2}{2}\right), & T < T_{AFD}, \\ 0, & T > T_{AFD}. \end{cases} \tag{4}$$

As one can see from the **Figure 2b-c** the heat capacity variation peculiarity appeared in the vicinity of AFM transition, that is break at $\chi = 0$, which becomes smeared and shifted with χ increase. At $\chi = 0$ and temperatures $T < T_N$ the heat capacity change is associated with the appearance of AFM order parameter, $L \approx \pm\sqrt{\alpha_{LT}(T_N - T)/\beta_L}$, in the immediate vicinity below the AFM order phase transition. At $\chi = 0$ and temperatures $T_N < T < T_S$ the parameter $L = 0$. Therefore under the absence of bilinear coupling between the sublattices magnetization and antiferrodistortive tilts, only the sharp jump appears on the specific heat at Neel temperature T_N. The jump value is equal to $\delta C_P^N = T_N(\alpha_{LT})^2/2\beta_L$.

Note that linear magnetoelectric effect (if one exists in a concrete antiferromagnet) does not contribute into the specific heat behaviour in the absence of external fields, and so the question about the contribution of other coupling, biquadratic e.g. antiferrodistortive-electric, magnetoelectric or antiferrodistortive-magnetic, to the specific heat smearing near T_N arises. If these or others contributions exist how they can be separated from the ones caused by the considered bilinear coupling? In order to answer the question let us estimate the contribution of the biquadratic couplings between different order parameters and their mean squire fluctuations into the specific heat of antiferrodistortive ferroelectric-antiferromagnet.

In order to calculate the contribution one can modify the free energy (2) by adding the ferroelectric contribution, $g_{FE} = \alpha_P(T)P^2 + \beta_p P^4$, and biquadratic couplings, $g_{BQ} = \xi\Phi^2 L^2 + \eta\Phi^2 P^2 + \lambda P^2 L^2$. Ferroelectric polarization leads to the occurrence of additional

term in Eq.(4), that is equal to $\delta C_P \approx -T \dfrac{d}{dT}\left(\dfrac{d\alpha_P}{dT}\dfrac{P^2}{2}\right)$ and nonzero in ferroelectric phase at temperatures $T < T_{FE}$.

Rigorously speaking the biquadratic terms can only shift corresponding transition temperatures, but cannot lead to any smearing of diffuseness in the transition region. Thus the smearing effect is related with the bilinear term $\chi L\Phi$ in thermodynamic limit.

Using Ginzburg-Levanuk approach [34] for the estimation of the order parameters mean square fluctuations contribution into the specific heat in the vicinity of AFM phase transition, we include the gradient terms in the free energy (2), which have the simplest form in the isotropic approximation, $g_{gr} = \dfrac{\gamma_\Phi}{2}(\nabla\Phi)^2 + \dfrac{\gamma_P}{2}(\nabla P)^2 + \dfrac{\gamma_L}{2}(\nabla L)^2$, and the entropy that density near AFM phase transition is approximately equal to $g_{fl}^{AFM} \approx \dfrac{k_B T}{2\pi^2}\int_0^{k_{max}} k^2 \ln\left(\alpha_{LT}\left|T - T_{AFM}\right| + \gamma_L k^2\right)dk$.

Corresponding expression for the order parameters fluctuations contribution into the specific heat change near AFM has the form [34]:

$$\delta C_P^{fl} \approx \frac{k_B T^2 \alpha_{LT}^{3/2}}{8\pi\gamma_L^{3/2}\sqrt{\left|T - T_{AFM}\right|}} \tag{5}$$

Expression (5) diverges at $T = T_{AFM}$ for finite γ_L due to the fluctuations, which contribution disappears in the limiting case $\gamma_L \to \infty$ (thermodynamic limit of Landau theory). Elementary estimations made for the typical values of parameters α_{LT}, β_L и γ_L [35], have shown, that the smearing effect defined in Eq. (5), is essential only in very narrow vicinity of antiferromagnetic phase transition (for temperatures interval from fractions of Kelvin to few Kelvin wide), while the experimentally observed range of specific heat jump smearing is of order of 20-50 Kelvin. Really, at $\chi=0$ the ratio $\dfrac{\delta C_P^{fl}}{\delta C_P^{N}} = \dfrac{k_B T^2 \beta_L}{4\pi\gamma_L^{3/2}T_N\sqrt{\alpha_{LT}\left|T - T_N\right|}}$ becomes less than 0.01 already at $\left|T - T_N\right| > 1$ K. Consideration of χ-effect Barret's law for temperature dependence of $\alpha_L(T)$ could not change significantly this estimation. Therefore, fluctuation (5) does not make a significant contribution to the smearing of the specific heat jump, observable in experiment, approving the conclusion that most of the smearing of AFM phase transition is associated with bilinear coupling $\chi L\Phi$ only.

Below we consider multiferroic $BiFeO_3$, which is antiferrodistive ferroelectric – antiferromagnet with critical temperatures $T_N \approx 645$ K, $T_C \approx 1100$ K and $T_S \approx 1200$ K [22]. Our fitting of temperature dependence of AFM order parameter L in $BiFeO_3$ obtained from neutron scattering experiment of Fischer et al [36] is shown **Figure 2a**. The fitting of temperature

dependence of specific heat and its part associated with transition to AFM phase is shown in **Figure 2b-c** for the experimental results of Kallaev et al [37].
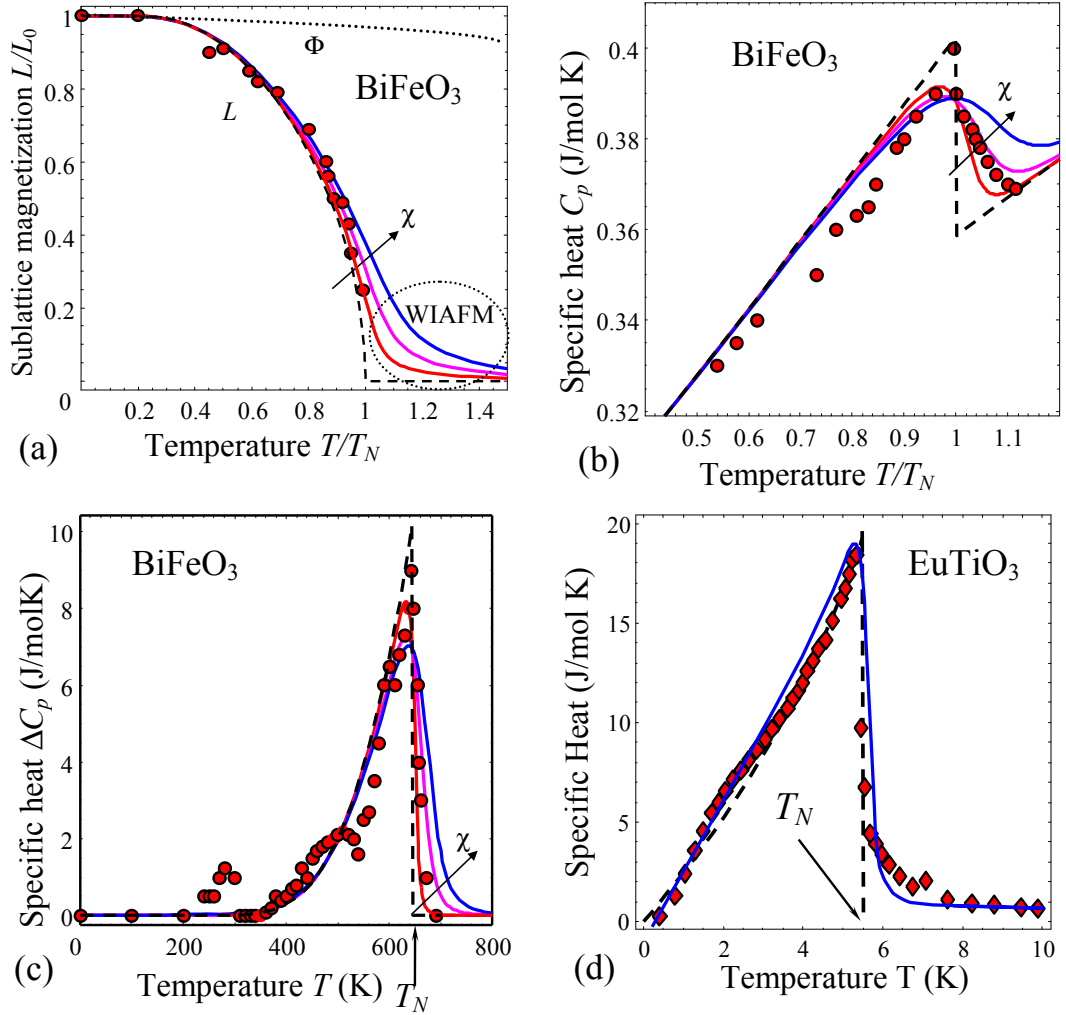
Figure 2. (a) Sublattices magnetization $L(T)/L(0)$ and **(b)** heat capacity variation as a function of reduced temperature T/T_N. Symbols are experimental data for BiFeO$_3$ from Fischer et al [36] on neutron scattering and Kallaev et al [37] for specific heat correspondingly. Curves are calculated by us for effective coupling constant $\widetilde{\chi} = 2$, 5, 10 SI units (solid curves) and $\chi = 0$ (dashed curve); $T_N = 645$ K, $T_L = 550$ K, $T_\Phi = 100$ K, $T_S = 1200$ K. Dotted curve in the plot **(b)** is the AFD order parameter, Φ/Φ_0, that is almost independent on χ value for chosen parameters. **(c)** Temperature dependencies of the anomalous contribution to the BiFeO$_3$ specific heat. Symbols are experimental data from [37]. Solid curves are calculated at $\widetilde{\chi} = 2$, 5, 10 SI units, dashed curves corresponds to $\chi = 0$. **(d)** Specific heat variation of EuTiO$_3$ near the AFM transition. Symbols represent the experimental data [30-32]. Effective coupling constant $\chi = 0$

10

(dashed curve) and $\widetilde{\chi} = 2$ SI units (solid curve); $T_N = 5.5$ K, $T_S = 285$ K. Other parameters of EuTiO$_3$ are listed in the Table 1 in the ref [15].

Solid curves from Fig.2 correspond to nonzero value of effective parameter $\widetilde{\chi} = (\chi/\beta_L)\sqrt{\alpha_{\Phi T}/\beta_\Phi} = 2, 5, 10$ SI units, dashed curves correspond to the case $\widetilde{\chi} = 0$. The best fitting was obtained for $\widetilde{\chi} = 2$ SI units. It is clearly seen that abrupt jumps of order parameter L temperature dependences, corresponding to the calculation at $\widetilde{\chi} = 0$, is in a satisfactory agreement with experimental points below T_N. The same situation is for the curve calculated at $\widetilde{\chi} = 2$ SI units, for which the small L exists above the Neel temperature, decreases with temperature increases and tends to zero at $T \to T_S$. However the specific heat features observed at $T = T_N$ are evidently blurred in the temperature region $T_N < T < 1.1 T_N$, at that the smearing can be satisfactory described only at $\widetilde{\chi} = 2$ SI units, but not at $\widetilde{\chi} = 0$. Therefore we can conclude that the diffuse "tail" of the antiferromagnetic order parameter L (as shown in the **Figure 2a**), that exists at nonzero $\widetilde{\chi}$ values, pointed out on the possibility of the "weak" ***improper*** antiferromagnetism (WIAFM) induced by the antiferrodistortive structural ordering.

To the best of our knowledge, the notion WIAFM is introduced here by us, and, naturally, requires explanations due to the possible muddle in the terminology related with its verbal similarity with a weak (anti)ferromagnetism. A weak ferromagnetism encounters rather often in various antiferromagnets and usually it is associated with the anticollinear spin canting. In many cases Dzialoshinski-Moriya (DM) interaction leads to the spin canting resulting in the appearance of a rather small total ferromagnetic moment M in an antiferromagnetic structure (see e.g. review [4] and refs therein). Sometimes weak ferromagnetism is called weak antiferromagnetism [38, 39]. However, the weak *improper* antiferromagnetism, which we predicted, should manifest itself in a different way than the aforementioned weak (anti)ferromagnetism. Actually, we predict the appearance of the small improper AFM order parameter "tail" that is proportional to the AFD order parameter and vanishes with the decrease of the AFD order under the temperature increase. No ferromagnetic moment exists in the considered case of weak improper antiferromagnetism, because the conjugated built-in field $\chi\Phi$ appears only in the equations for AFM order parameter L, namely $\alpha_L L + \beta_L L^3 + \xi^L_{RM} L\Phi^2 = -\chi\Phi$, while the equation for M remains homogeneous without external magnetic field, $\alpha_M M + \beta_M M^3 = 0$, and thus has only zero solution. The AFM order parameter becomes induced by the built-in the field $\chi\Phi$. Corresponding region of the WIAFM existence is schematically shown by a dotted ellipse in the **Figure 2a.**

Nothing definite can be concluded about the $\tilde{\chi}$ value from the analyses of the experimental data shown in the **Figure 2a**, because it is extremely complex to register relatively small sublattices magnetization values by neutron scattering. On the other hand it is evident from the specific heat behavior shown in the **Figure 2b-c**, that the inequality $\left|\tilde{\chi}\right| > 1$ SI units is necessary for the satisfactory agreement with experiment. Heat capacity variation of $EuTiO_3$ near the AFM transition is shown for comparison in the **Figure 2d**. As one can see from the plot nonzero $\tilde{\chi}$ (solid curve) describes the experimental data better than $\chi = 0$ (dashed curve). It is worth to underline that the smearing of sublattice magnetization and specific heat for $BiFeO_3$ and $EuTiO_3$ shown in **Figs.2** looks like the smearing of ferroelectric properties in external electric field [40]. This obviously confirmed the statement that the terms $\chi\Phi$ and χL can be considered as built-in fields in the lattices.

In the next section we show how the existence of antiferrodistortive-antiferromagnetic coupling can be approved from the specific heat behavior in the $BiFeO_3$-based solid solutions, and estimate the effect value.

4. Determination of the antiferrodistortive-antiferromagnetic coupling constant for $Bi_{1-x}R_xFeO_3$ solid solutions

Available experimental results demonstrate noticeable features of the temperature dependencies of the specific heat in $Bi_{1-x}R_xFeO_3$ (R=La, Nd, x=0 – 0.2) solid solutions [41]. The features appears at the temperature of the antiferromagnetic phase transition that is about (640-650) K. Corresponding experimental results are shown by symbols in the **Figures 3.** As one can see from the figure dashed curves calculated at $\tilde{\chi} = 0$ and different composition x do not describe the specific hear smearing at temperatures $T > T_N$. Solid curves, calculated as $\tilde{\chi} = (2 - 2.5)$ SI units and $T_N = (645 - 655)$ K in dependence of x, describe the smearing effect adequately, proving the importance of the bilinear antiferrodistortive-antiferromagnetic effect for the understanding of the specific heat behaviour near the antiferromagnetic phase transition. The inclusion of the bilinear antiferrodistortive-antiferromagnetic effect is necessary for the quantitative description of the experimental data.
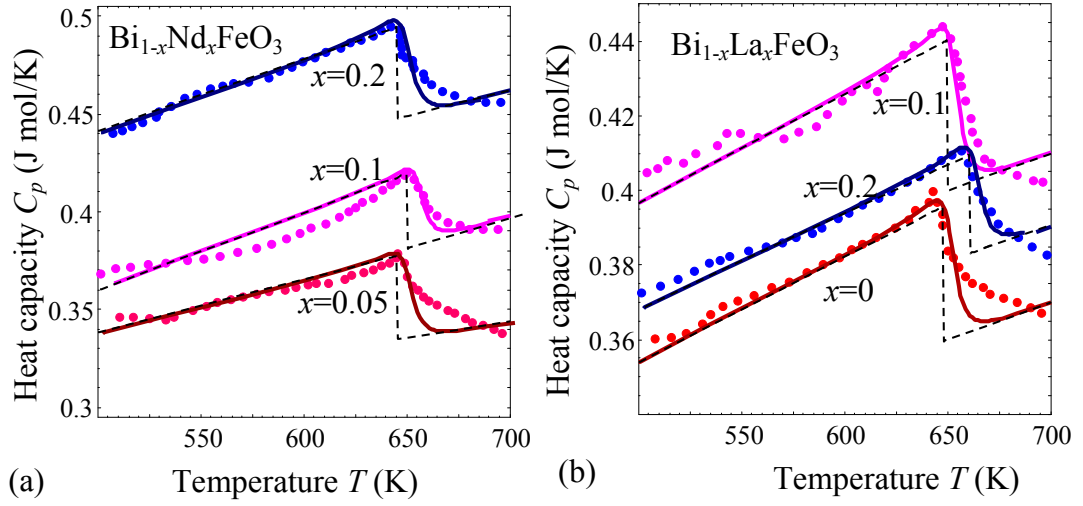
Figure 3. Temperature dependence of the specific heat near AFD phase transition of the solid solutions $Bi_{1-x}R_xFeO_3$ (R=La, Nd, x= 0 – 0.2). Symbols are experimental data for $Bi_{1-x}R_xFeO_3$ from Amirov et al [41] for heat capacity correspondingly. Dashed curves are calculated by us for dimensionless coupling constant $\tilde{\chi} = 0$. Solid curves correspond to different nonzero $\tilde{\chi} = (2 - 2.5)$ SI units and $T_N = (645 - 655)$ K depending on the composition x, $T_L = 550$ K, $T_\Phi = 100$ K, $T_S = 1200$ K.

Notice that we did not aimed to determine all material parameters of $Bi_{1-x}R_xFeO_3$ from the fitting of the specific heat variation $\delta C_p(T)$ and normalized antiferromagnetic order parameter $L(T)/L(0)$ temperature dependences, because it was impossible. Only the ratio $(\alpha_{LT})^2/2\beta_L$ can be defined from specific heat jump δC_p^N, and the temperature dependence of the ratio $\alpha_L(T)/\alpha_{LT}$ can be determined from the temperature dependence $L(T)/L(0)$. In order to define the value of α_{LT} one needs the temperature dependence of the antiferromagnetic susceptibility that we could not found in literature. Despite the difficulty we reached our goal and found the effective value of the antiferrodistortive-antiferrodistortive coupling constant, $\tilde{\chi} = (\chi/\beta_L)\sqrt{\alpha_{\Phi T}/\beta_\Phi}$, from the fitting of experimental data.

5. Conclusions

The possibility of the linear antiferrodistortive-antiferromagnetic effect existence in perovskite-multiferroics with the structural formula AMO_3, antiferrodistive and antiferromagnetic ordering is demonstrated. Within the framework of the theory of symmetry and the microscopic model the necessary conditions for this effect occurrence are the simultaneous change in the sign of the corresponding components of the elementary

magnetization vectors in the neighboring antiferromagnetic sublattices coupled with the change of the antiferrodistive displacement direction in the neighboring oxygen octahedron MO_6. Let us underline that the trilinear antiferrodistortive-antiferromagnetic coupling should appear simultaneously with the considered bilinear antiferrodistortive-antiferromagnetic coupling, as well as higher odd order couplings of the type.

Physical manifestations of antiferrodistortive-antiferromagnetic effect is smearing of the antiferromagnetic phase transition and the emergence of small "improper" antiferromagnetic order parameter L above the Neel temperature and below the temperature of antiferrodistortive transition. The parameter L is induced by the product of the AFD order parameter Φ on the antiferrodistortive-antiferromagnetic coupling constant χ, at that the term $\chi\Phi$ acts as effective built-in conjugated field for the parameter. Therefore, there is the possibility to observe weak "improper" antiferromagnetism induced by the structural antiferrodistive ordering Φ above the Neel temperature. For example, in bismuth ferrite, for which the antiferromagnetic transition temperature is of the order of (640-655) K, and the temperature antiferrodistortive transition goes above 1200 K, the temperature dependence of L was measured by neutron scattering method. However, the available experimental data cannot say anything definite about the value of a smearing effect, because it is extremely difficult to register a sufficiently small value of L by neutron scattering.

Antiferrodistortive-antiferromagnetic effect also leads to the smearing of the jump of the specific heat near the temperature of antiferromagnetic phase transition. By quantitative comparison with experiments we made estimates of the linear effect in antiferromagnetic solid solutions of multiferroic $Bi_{1-x}R_xFeO_3$ and determine the optimal value of the antiferrodistortive-antiferromagnetic coupling constants from the fitting to experimental data. Calculated dependencies describe the experiment quite satisfactory, thus proving the importance of bilinear antiferrodistortive-antiferromagnetic effect for the understanding of the mechanisms responsible for the temperature dependence of the specific heat behaviour near the antiferromagnetic phase transition.

References

1 M. Fiebig. "Revival of the magnetoelectric effect." Journal of Physics D: Applied Physics **38**, R123 (2005).

2 N. A. Spaldin and M. Fiebig, "The renaissance of magnetoelectric multiferroics." Science **309**, 391-392 (2005).

3 J.M. Rondinelli, N.A. Spaldin. "Structure and properties of functional oxide thin films: insights from electronic structure calculations." Advanced Materials **23**, 3363 (2011).

4 A. P., Pyatakov, A. K.Zvezdin, "Magnetoelectric and multiferroic media." Physics-Uspekhi, **55**(6), 557 (2012).

5 J. F. Scott. "Data storage: Multiferroic memories." Nature materials **6**, 256-257 (2007).

6 V.G. Bar'yakhtar, V.A. L'vov, D.A. Yablonskii. "Inhomogeneous magnetoelectric effect." JETP Lett. **37**, 673 (1983).

7 Maxim Mostovoy, "Ferroelectricity in spiral magnets." Phys. Rev. Lett. **96**, 067601 (2006).

8 A. Sparavigna, A. Strigazzi, and A. Zvezdin, "Electric-field effects on the spin-density wave in magnetic ferroelectrics."Phys. Rev. **B 50**, 2953 (1994).

9 A.P. Pyatakov and A.K. Zvezdin, "Flexomagnetoelectric interaction in multiferroics." Eur. Phys. J. B **71**, 419 (2009).

10 B.M. Tanygin. "Symmetry theory of the flexomagnetoelectric effect in the magnetic domain walls." Journal of Magnetism and Magnetic Materials **323**, 616 (2011).

11. E.A. Eliseev, M.D. Glinchuk, V. Khist, V.V. Skorokhod, R. Blinc, A.N. Morozovska. "Linear magnetoelectric coupling and ferroelectricity induced by the flexomagnetic effect in ferroics." Phys.Rev. B 84, 174112 (2011)

12. Morozovska, Anna N., Eugene A. Eliseev, Maya D. Glinchuk, Long-Qing Chen, and Venkatraman Gopalan. "Interfacial polarization and pyroelectricity in antiferrodistortive structures induced by a flexoelectric effect and rotostriction." Physical Review **B 85**, 094107(2012).

13. Eugene A. Eliseev, Sergei V. Kalinin, Yijia Gu, Maya D. Glinchuk, Victoria Khist, Albina Borisevich, Venkatraman Gopalan, Long-Qing Chen, and Anna N. Morozovska. "Universal emergence of spatially modulated structures induced by flexoantiferrodistortive coupling in multiferroics." Phys.Rev. B **88**, 224105 (2013).

14 Venkatraman Gopalan, and Daniel B. Litvin. "Rotation-reversal symmetries in crystals and handed structures." Nature Materials **10**, 376 (2011).

15 Eugene A. Eliseev, Maya D. Glinchuk, Venkatraman Gopalan, Anna N. Morozovska. "Rotomagnetic couplings influence on the magnetic properties of antiferrodistortive antiferromagnets" http://arxiv.org/abs/1409.7108

16. Hiromoto Uwe, and Tunetaro Sakudo. "Stress-induced ferroelectricity and soft phonon modes in SrTi O 3." Physical Review **B 13**, 271 (1976).

17. M. J. Haun, E. Furman, T. R. Halemane and L. E. Cross, "Thermodynamic theory of the lead zirconate-titanate solid solution system, part IV: tilting of the oxygen octahedra." Ferroelectrics **99**, 55 (1989)

18. B. Houchmandzadeh, J. Lajzerowicz and E Salje, "Order parameter coupling and chirality of domain walls."J. Phys.: Condens. Matter **3**, 5163 (1991).

19. E.V. Balashova and A.K. Tagantsev, "Polarization response of crystals with structural and ferroelectric instabilities." Phys. Rev. B 48, 9979 (1993).

20. A.K. Tagantsev, E. Courtens and L. Arzel, "Prediction of a low-temperature ferroelectric instability in antiphase domain boundaries of strontium titanate." Phys. Rev. B, **64**, 224107 (2001).

21. M.D. Glinchuk, E.A. Eliseev, A.N. Morozovska, R. Blinc. "Giant magnetoelectric effect induced by intrinsic surface stress in ferroic nanorods." Phys. Rev. **B 77**, 024106-1-11 (2008)

22 Gustau Catalan, James F. Scott, "Physics and applications of bismuth ferrite." Adv. Mater. **21**, 1–23 (2009)

23 G. A. Smolenskii, L. I. Chupis, "Ferroelectromagnets." Sov. Phys. Usp. **25**, 475 (1982).

24 L.D. Landau, E.M. Lifshitz, L. P. Pitaevskii. Electrodynamics of Continuous Media, (Pergamon Press, Oxford, New-York, Beijing, Frankfurt, 1984), p.176, §51 "Piezomagnetism and the magnetoelectric effect"

25 B. A. Tavger and V. M. Zaitsev, Magnetic symmetry of crystals. Z. Exp. Theor. Phys. **30**, 564 (1956) [*Sov. Phys. JETP-USSR* 3, no. 3 (1956): 430-436.].

26 G. T. Rado and V. J. Folen, "Magnetoelectric Effects in Antiferromagnetics." Journal of Applied Physics **33**, 1126 (1962).

27 G.A. Smolenskii, V.A. Bokov, V.A. Isupov, N.N Krainik, R.E. Pasynkov, A.I. Sokolov, *Ferroelectrics and Related Materials* (Gordon and Breach, New York, 1984). P. 421

28 A. M. Kadomtseva, A. K. Zvezdin, Yu. F. Popov, A. P. Pyatakov, G. P. Vorob'ev. "Space-time parity violation and magnetoelectric interactions in antiferromagnets" Journal of Experimental and Theoretical Physics Letters 79, Issue 11, pp 571-581 (2004). Doi: 10.1134/1.1787107

29 J. H. Barrett, "Dielectric constant in perovskite type crystals." Phys. Rev. **86**, 118 (1952).

30 T. Katsufuji and H. Takagi, "Coupling between magnetism and dielectric properties in quantum paraelectric EuTiO 3." Phys. Rev. B **64**, 054415 (2001).

31 V. V. Shvartsman, P. Borisov, W. Kleemann, S. Kamba, T. Katsufuji. "Large off-diagonal magnetoelectric coupling in the quantum paraelectric antiferromagnet EuTiO 3." Phys. Rev. B **81**, 064426 (2010).

32 P. G. Reuvekamp, R. K. Kremer, J. Kohler, and A. Bussmann-Holder. "Spin-lattice coupling induced crossover from negative to positive magnetostriction in EuTiO 3." Phys. Rev. B **90**, 094420 (2014)

33 See Supplemental Material at [URL will be inserted by publisher] for details of calculations.

34 B. A. Strukov and A. P. Levanyuk, *Ferroelectric Phenomena in Crystals* (Springer, Berlin, 1998)

35 k_B=1.38×10^{-23} J/K, α_{TP} = 4.366·10^{-7}, T_N = 650 K, β_P = 0.323*10^{-17}, γ_{LP} = 10^{-8} m^3/F

36 P. Fischer, M. PoIomska, I. Sosnowska, M. Szymanski "Temperature dependence of the crystal and magnetic structures of BiFeO3."J. Phys. C: Solid St. Phys., **13**, 1931-1940 (1980).

37 S. N. Kallaev, Z. M. Omarov, R. G. Mitarov, A. R. Bilalov, G. G. Gadzhiev, L. A. Reznichenko, R. M. Ferzilaev, S. A. Sadykov, "Heat capacity and dielectric properties of multiferroics Bi1− x Gd x FeO3 (x= 0–0.20)." Physics of the Solid State 56, Issue 7, pp 1412-1415 (2014)

38 S. Doniach. „The Kondo lattice and weak antiferromagnetism." Physica B+C, **91**, 231–234 (1977)

39 S. Fujiyama, K. Ohashi, H. Ohsumi, K. Sugimoto, T. Takayama, T. Komesu, M. Takata, T. Arima, and H. Takagi. „Weak antiferromagnetism of *J*eff =1/2 band in bilayer iridate Sr3Ir2O7." Phys.Rev. B **86**, 174414 (2012)

40 M. E. Lines and A. M. Glass, *Principles and Application of Ferroelectrics and Related Materials* (Clarendon Press, Oxford, 1977).

41 A. A. Amirov, A. B. Batdalov, Z. M. Omarov, S. N. Kallaev, I. A. Verbenko, L. A. Reznichenko, The heat capacity of multiferroic Bi1-xRexFeO3 (Re = La, Nd; x = 0-0,2) Phase transitions, ordered states and new materials Number 03 (2010). URL: http://ptosnm.ru/ru/issue/2010/3/48/publication/514